The luminescence parameters of Yb3+:Er3+ – doped LiLa(WO4)2 single crystal grown in the form of fiber for up-conversion…

Article *in* Journal of Luminescence · July 2017

DOI: 10.1016/j.jlumin.2017.03.072

4 authors, including:

Rafael Lima Denaldi
Instituto de Pesquisas Energéticas e Nucleares
1 PUBLICATION **0** CITATIONS
SEE PROFILE

Jair Ricardo De Moraes
Galileo Gymnasium
22 PUBLICATIONS **21** CITATIONS
SEE PROFILE

Sonia Licia Baldochi
Instituto de Pesquisas Energéticas e Nucleares
154 PUBLICATIONS **1,065** CITATIONS
SEE PROFILE

Journal of Luminescence 187 (2017) 479–485

Contents lists available at ScienceDirect

Journal of Luminescence

journal homepage: www.elsevier.com/locate/jlumin

The luminescence parameters of Yb^{3+}:Er^{3+}-doped $LiLa(WO_4)_2$ single crystal grown in the form of fiber for up-conversion green emission

Laercio Gomes*, Rafael Lima Denaldi, Jair Ricardo de Moraes, Sonia Licia Baldochi

Center for Lasers and Applications, IPEN/CNEN-SP, P.O. Box 11049, São Paulo, SP 05422-970, Brazil

A B S T R A C T

This report details the first study of the luminescence properties of a single crystal grown in the form of fiber for prospective application as the gain medium for fiber laser emission at 552 nm. The excited state decay processes related with the $^4S_{3/2}\rightarrow{}^4I_{15/2}$ transition in double Yb^{3+}:Er^{3+}-doped $LiLa(WO_4)_2$ crystal have been investigated using time-resolved fluorescence spectroscopy with a Er^{3+} concentration of 0.5 mol% and Yb^{3+} with 2, 5, 7, 10 and 15 mol%. Selective laser excitation of the $^2F_{5/2}$ energy level of Yb^{3+}(972 nm) and selective laser excitations of the $^4I_{11/2}$ and $^4I_{13/2}$ energy levels of Er^{3+}(972 and 1550 nm), respectively has established that in a similar way to other optical materials, a strong energy-transfer up-conversion by way of a dipole-dipole interactions between an Yb^{3+} excited and Er^{3+} ions, the $^4F_{5/2}$ level (Yb^{3+}) populates the $^4S_{3/2}$ upper laser level of the 550 nm transition. The $^4S_{3/2}$ energy level emits luminescence with peaks having the wavelength center at 550 nm with luminescence efficiency increasing from 7% for Er^{3+} singly doped to 36% for Yb^{3+}(15 mol%) co-doped crystals. The $^4S_{3/2}$ lifetime of Er^{3+} is observed to increase due to the saturation of the multiphonon relaxation rate at high excited-state density of Yb^{3+} ions. At high excited-state density, Yb^{3+} ions saturates the accepting modes inside of a critical volume of $R_C = 39.4$ Å centered at an excited Er^{3+}($^4S_{3/2}$) ion, by the high-energy phonons generated from emission sideband of Yb^{3+} ions in Yb(x%):Er(0.5%) crystals. It is established that the green (552 nm) up-conversion luminescence of Er^{3+} is optimized using an Yb^{3+} concentration of 11.5 mol% for Er(0.5%):$LiLa(WO_4)_2$ crystal.

1. Introduction

Efficient up-conversion lasers based on RE^{3+}-doped crystals with emission at wavelengths in the visible, green to blue spectral region, are very rare and new materials are needed for development of more compact all solid state lasers pumped by IR diode lasers. Several solid optical materials have been used to demonstrate the up-conversion luminescence mainly based on the use of Yb^{3+} ions as sensitizers. The use of high Yb^{3+} concentration ~10 mol% and small activators concentration as Er^{3+} ions have proportioned strong visible emission under Yb^{3+} ions excitation around 972 nm where powerful diode lasers are available today. Whilst a number of Yb:Er optical materials have demonstrated visible up-conversion luminescence and few of them have been operated efficiently [1,2], more luminescence spectroscopic investigation must be carried out to find new optical materials having more efficient green emission of Er^{3+} to develop up-conversion lasers.

To explore the potential of the $^4S_{3/2}\rightarrow{}^4I_{15/2}$ transition of the Er^{3+} ion that emits at 552 nm in Er^{3+}/Yb^{3+}- doped $LiLa(WO_4)_2$ crystal and more broadly to investigate the possibility of an efficient laser operating at 552 nm using a fiber single crystal, detailed spectroscopic studies are required. In this report, we investigate the luminescence properties of Er^{3+}/Yb^{3+}-doped $LiLa(WO_4)_2$ single crystal grown in the form of fiber by the micro-pulling down technique [3]. We carry out the basic spectroscopic measurements and assess the suitability of this optical material for emission in the visible. The luminescence efficiency of these levels was determined when the experimental decay time was compared with the radiative lifetimes reported in the literature. The multiphonon decay and the cross-relaxation (Er × Er) rates involving the $^4S_{3/2}$ in the host $LiLa(WO_4)_2$ were observed to be very weak compared to the radiative decay rate (or negligible) of $^4S_{3/2}$ excited level and perhaps this level was taken as full luminescence efficiency. Measurements of the up-conversion luminescence transient (green emission) enable to calculate the energy transfer up-conversion rate (U_P) parameters.

2. Experimental procedure

For this study, we grew five Er (0.5%): $LiLa(WO_4)_2$ single crystals in

* Corresponding author.
E-mail address: lgomes@ipen.br (L. Gomes).

http://dx.doi.org/10.1016/j.jlumin.2017.03.072
Received 28 November 2016; Received in revised form 3 March 2017; Accepted 29 March 2017
Available online 02 April 2017

the form of fibers that were co-doped with Yb (x%), where x = 0, 2, 5, 10 and 15 mol%. The fiber crystals were grown with lengths up to 20 mm and constant diameters of 1.0 mm using an oriented fiber seed having the c-axis in the plane perpendicular to the fiber length. All the experiments were performed using a resistive micro pulling down furnace, in an air atmosphere, with pulling rate of 0.15 mm/min. The Er^{3+} ion density in the sample was calculated to be 5×10^{19} cm^{-3} for the doped $LiLa(WO_4)_2$ sample with 0.5 mol% from X-ray fluorescence measurement.

The decay characteristics of the excited states of Er^{3+} were measured using pulsed (typically 10 mJ, 4 ns, 10 Hz) laser excitation from a tunable optical parametric oscillator (OPO) pumped by the second harmonic of a *Q*-switched Nd-YAG laser (Brilliant B from Quantel). Tunable laser excitation from the OPO was used to directly excite the $^2F_{7/2}$ energy levels of the Yb^{3+} ion at 972 nm. The infrared luminescence ($\lambda > 1100$ nm) was detected using an InSb infrared detector (Judson model J-10 D cooled to 77 K) in conjunction with a fast preamplifier, with a response time of approximately 0.5 μs, and analyzed using a digital 200 MHz oscilloscope (Tektronix TDS 410). The visible and near infrared ($\lambda < 1100$ nm) was detected using a photomultiplier tube (EMI) with a sensitive cathode of S-1 type (or S-20) (PMT EMI refrigerated at −20 °C) with a response time of 10 ns. All the fluorescence decay characteristics were measured at 300 K. To isolate the infrared luminescence signals, band pass filters each with ~80% transmission at 1600 and 2750 nm with a half width of 25 nm and an extinction coefficient of approximately 10^{-5} outside this band were used. Luminescence spectra were measured using an HR 2000-VIS CCD fiber spectrometer (fiber diameter of 100 μm) from Ocean Optics with an optical resolution of 0.8 nm.

3. Experimental results

When Yb^{3+}:Er^{3+}-doped $LiLa(WO_4)_2$ crystal is excited at 972 nm, the main processes involving the energy levels are, see Fig. 1: (a) Yb^{3+} ground state absorption (GSA), $^2F_{7/2}+h\nu$ (972 nm)→$^2F_{5/2}$ and Er^{3+} ground state absorption (GSA) $^4I_{15/2}$ (Er^{3+})+hν (972 nm)→$^4I_{11/2}$ (Er^{3+}); (b) energy transfer up-conversion (U_{P1}), $^2F_{5/2}$ (Yb^{3+})+$^4I_{15/2}$ (Er^{3+})→$^2F_{7/2}$ (Yb^{3+})+$^4I_{11/2}$ (Er^{3+}) (U_{P1a}) and $^2F_{5/2}$ (Yb^{3+})+$^4I_{11/2}$ (Er^{3+})→$^2F_{7/2}$ (Yb^{3+})+$^4F_{7/2}$ (Er^{3+}) (U_{P1b})→$^4S_{3/2}$+ $\hbar w$; (c) energy transfer up-conversion (U_{P2}), $^2F_{5/2}$ (Yb^{3+})+$^4I_{11/2}$ (Er^{3+})→$^2F_{7/2}$ (Yb^{3+})+$^4F_{7/2}$ (Er^{3+})→$^4S_{3/2}$+ $\hbar w$; (d) Er^{3+} excited state absorption (ESA), $^4I_{11/2}+h\nu$ (972 nm)→$^4F_{7/2}$→$^4S_{3/2}$+ $\hbar w$. The term $\hbar w$ relates to the phonon energy of the crystal ($\hbar w = 880$ cm^{-1}). Radiative transition rates of the main transitions of Er^{3+} in $LiLa(WO_4)_2$ were calculated using Judd-Ofelt theory and the parameters values experimentally obtained for the main luminescence levels are listed in Table 1. In these calculations the intensity parameters $\Omega_2 = 9.02\times10^{-20}$ cm^2, $\Omega_4 = 2.02\times10^{-20}$ cm^2 and $\Omega_6 = 0.59\times10^{-20}$ cm^2 were taken from the literature [4]. For an electric dipole transition, the reduced matrix elements $U^{(\lambda)}$ for Er^{3+}, which are considered to vary only slightly from host to host, were considered unchanged, so we used the values from the literature [5].

3.1. Upconversion emission of Er^{3+} in single Er- and Yb-codoped crystals

The emission spectrum from the Er^{3+}(0.5%) -doped $LiLa(WO_4)_2$ single crystal grown in the form of fiber was obtained using the HR 2000-VIS spectrometer coupled to the optical fiber bundle to collect the luminescence signal using a pulsed laser excitation at 972 nm. The measured luminescence spectra were corrected from the spectral response of the equipment (optical grating efficiency). The up-conversion luminescence spectrum was induced by up-conversion energy transfer where two excited Er^{3+} ions in the $^4I_{11/2}$ interact to promote the population of the upper excited level $^2H_{11/2}$ that decays to the $^4S_{3/2}$ luminescent level. The up-conversion emission spectrum measured for the Yb(x%):Er(0.5%): $LiLa(WO_4)_2$ single crystals (fiber) are shown in the Fig. 2, where the visible luminescence was induced by the laser excitation at 972 nm. The main up-conversion emissions are due to the $^4S_{3/2}$→$^4I_{15/2}$ (centroid at 550 nm), $^2H_{11/2}$→$^4I_{15/2}$ (527 nm) and $^4F_{9/2}$→$^4I_{15/2}$ (653 nm) transitions.

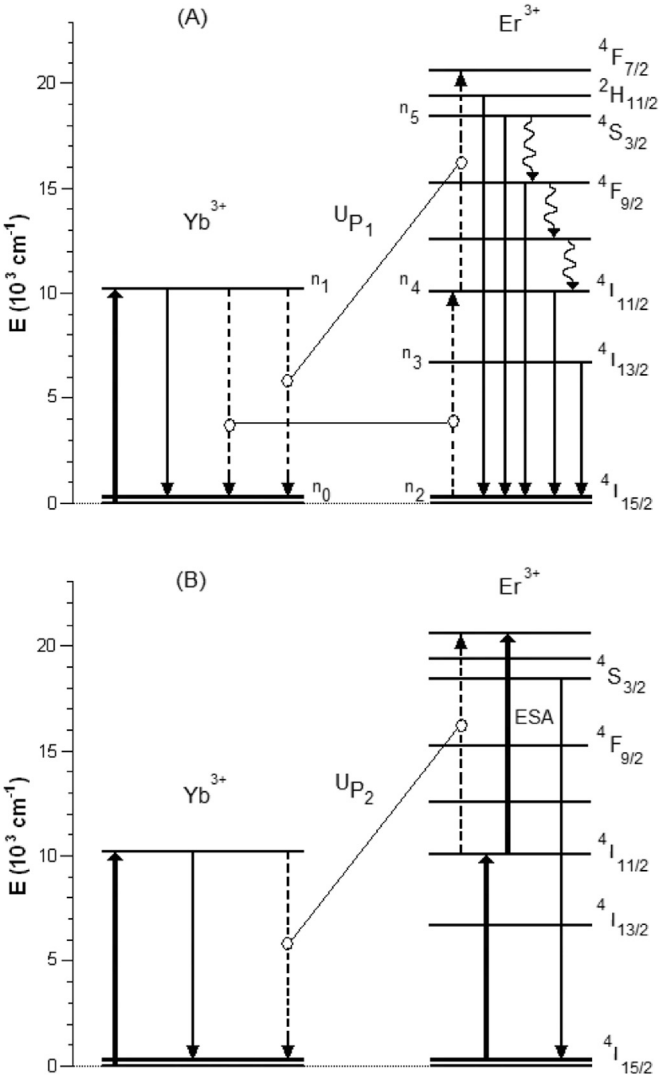

Fig. 1. Energy level scheme showing the pump laser, energy transfer mechanisms relevant to the laser operation at 556 nm. Solid line (up): 972 nm excitation. Solid lines (down): Er^{3+} emissions (at 550, 653, 980, 1537 nm). Dashed lines (up and down): U_{P1}, U_{P2} and ESA processes. Fig. 1(A) shows the up-conversion (U_{P1}) process in details what is more effective for [Yb] > 5 mol%; Fig. 1(B) shows the ESA absorption and U_{P2} process, which are competing process to produce the up-conversion luminescence when the [Yb] concentration is between 2 and 5 mol%. n_0 and n_1 are the ground ($^2F_{7/2}$) and excited ($^2F_{5/2}$) state populations of Yb^{3+} ions. n_2 and n_5 are the ground ($^4I_{15/2}$) and excited ($^4S_{3/2}$) states populations of Er^{3+} ions.

3.2. Luminescence decays from the $^4S_{3/2}$, $^4I_{11/2}$ and $^4I_{13/2}$ excited levels of Er^{3+}

When the sample was excited at 972 nm both Yb^{3+} and Er^{3+} are excited and the luminescence at 527, 550 and 653 nm are observed from the $^2H_{11/2}$, $^4S_{3/2}$ and $^4F_{9/2}$ excited states of Er^{3+} strongly due to U_{P1} (or U_{P2}) up-conversion processes shown in a schematic diagram of Fig. 1. Laser excitation at 972 nm also produces ESA (excited state absorption) from the $^4I_{11/2}$ excited level of Er^{3+} as shown in diagram of Fig. 1(b). The best fit to the temporal decay characteristics relevant to the $^4S_{3/2}$ energy decay, when directly excited by one photon or ESA absorption, was accurately described by the experimental decay function given by Eq. (1)

Table 1
Radiative transition rate, branching ratio and radiative lifetime of Er^{3+} calculated in this work for Er^{3+} in $LiLa(WO_4)_2$ crystal. The refractive index, n = 2 was used in calculations.

Transition (Er^{3+})	Wavelength $\bar{\lambda}$ (nm)	Radiative Rate A_{ed} (s^{-1})	β	τ_R (ms)
$^2H_{11/2}$ →				0.042
$^4I_{15/2}$	527	23905	0.960	
$^4S_{3/2}$ →				0.556
$^4I_{9/2}$	1679	91	0.050	
$^4I_{11/2}$	1222	43	0.024	
$^4I_{13/2}$	846	491	0.273	
$^4I_{15/2}$	550	1173	0.653	
$^4F_{9/2}$ →				0.324
$^4I_{11/2}$	1981	102	0.033	
$^4I_{13/2}$	1152	44	0.040	
$^4I_{15/2}$	653	2945	0.953	
$^4I_{11/2}$ →				3.72
$^4I_{13/2}$	2750	24	0.088	
$^4I_{15/2}$	974	245	0.912	
$^4I_{13/2}$ →				6.92
$^4I_{15/2}$	1537	145	1	

$\Omega_2 = 9.02\times10^{-20}\ cm^2$, $\Omega_4 = 2.02\times10^{-20}\ cm^2$ and $\Omega_6 = 0.59\times10^{-20}\ cm^2$ were obtained from Ref. [4].

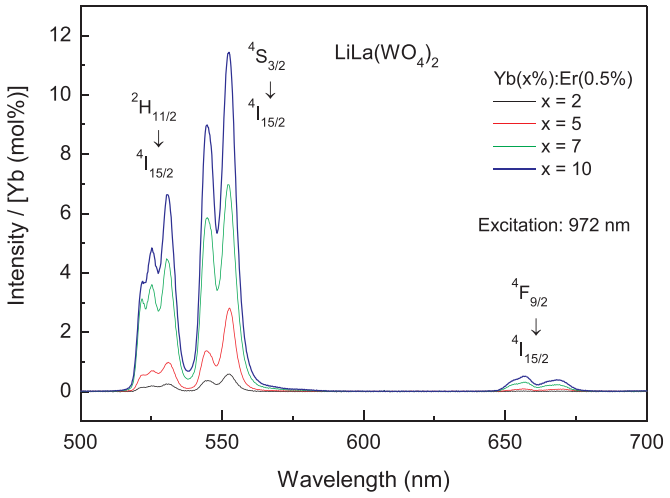

Fig. 2. Up-conversion emission spectrum of Er^{3+} in Yb(x):Er(0.5):$LiLa(WO_4)_2$ single crystal (fiber) with x = 2%, 5%, 7% and 10% measured after pulsed laser excitation at 972 nm with an average energy of 10 mJ. The emission intensity was normalized by the Yb^{3+}(x mol%) concentration for comparison.

$$I(t) = I_0 \exp\left(-\gamma\sqrt{t} - \frac{t}{\tau_d} - \overline{W}t\right), \quad (1)$$

where $\tau_d = \frac{\tau_R}{1 + W_{NR}\tau_R}$ is the intrinsic decay of donor, τ_R is the radiative decay of donor and W_{NR} is the multiphonon decay rate (donor). The non-exponential term exp(-γ√t), called the classical Förster decay function, describes energy transfer (D→A) processes without energy migration through donor states, also known as static disordered decay involving the dipole-dipole interaction [6]. γ ($s^{-1/2}$) is the energy transfer parameter (cross-relaxation (CR) or energy-transfer by up-conversion (ETU)). The last exponential term $\exp(-\overline{W}t)$ in Eq. (1) describes energy transfer (D→A) processes enhanced by energy migration. Considering a non-exponential decay of donor, the mean lifetime (τ) of donor excitation can be obtained by the integration of decay curve (Eq. (2)) using

$$\tau = \frac{1}{I_0}\int_0^\infty I(t)dt. \quad (2)$$

Eq. (1) was rewritten in order to have two fitting parameters, t_1 and γ giving

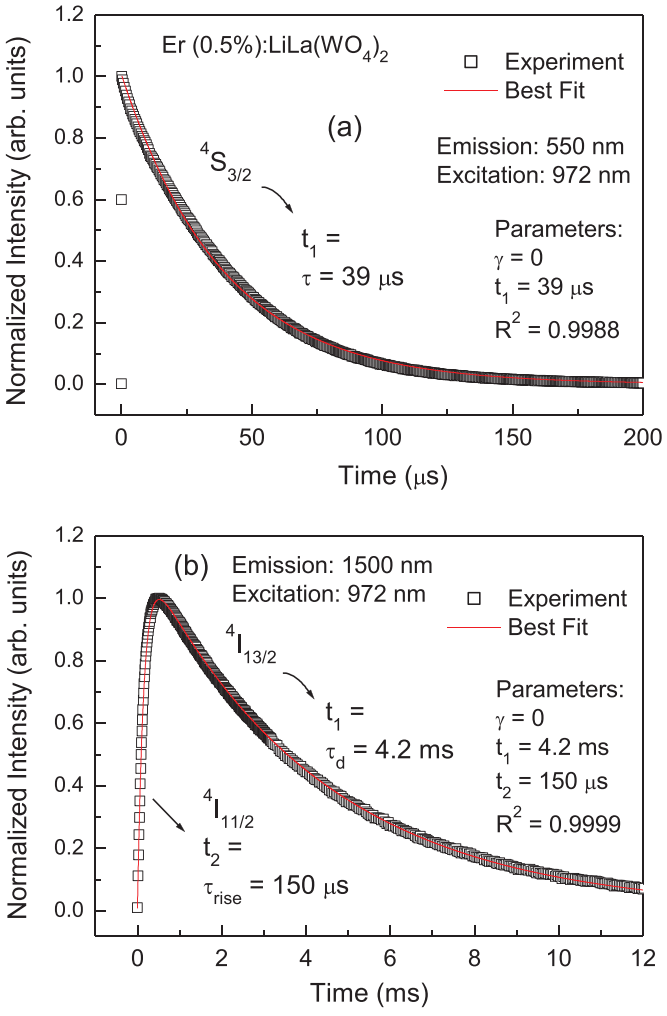

Fig. 3. Emission decay curves measured at 550 nm ($^4S_{3/2}$→$^4I_{15/2}$) (a) and at 1500 nm ($^4I_{13/2}$→$^4I_{15/2}$) after laser excitation at 972 nm in Er(0.5%):$LiLa(WO_4)_2$ crystals. The $^4S_{3/2}$ level (a) was excited by ESA (excited state absorption) process. The risetime of the 1500 nm emission (b) is due to the $^4I_{11/2}$→$^4I_{13/2}$ emission decay.

$$I(t) = I_0 \exp\left(-\gamma\sqrt{t} - \frac{t}{t_1}\right), \quad (3)$$

where $t_1 = \frac{\tau_d}{1 + \tau_d \overline{W}}$.

Because the luminescence of $^4F_{9/2}$ level is excited by the non-radiative multiphonon decay from the upper level ($^4S_{3/2}$) we use an experimental function that precisely describes the luminescence transient given by Eq. (4)

$$I(t) = I_0[\exp(-\gamma_1\sqrt{t} - t/t_1) - \exp(-t/t_2)], \quad (4)$$

where I_0 is the initial amplitude, γ_1 and t_1 are the fitting parameters of $^4S_{3/2}$ level decay and t_2 is the time decay of the $^4F_{9/2}$ level.

Lifetime of $^4S_{3/2}$, $^4F_{9/2}$, $^4I_{11/2}$ and $^4I_{13/2}$ levels of Er^{3+} in single doped $LiLa(WO_4)_2$ crystal fiber were measured using pulsed laser excitation at 972 nm with and an average energy of 8 mJ with an approximate excitation pump power of 35 MW cm^{-2}. Besides this high excitation pump power used in the luminescence measurements we did not see any thermal and nonlinear effects on the measurements. The experimental emission decays of $^4S_{3/2}$ and $^4I_{13/2}$ levels are seen in Fig. 3(a) and (b), respectively. The emission decay of $^4F_{9/2}$ level is indirectly excited by ESA at 972 nm is seen in Fig. 4. Best fits of the emission decays were performed using Eq. (4) (or Eq. (3) for the $^4S_{3/2}$ decay) and the best-fitted parameters and lifetimes are given in Table 2.

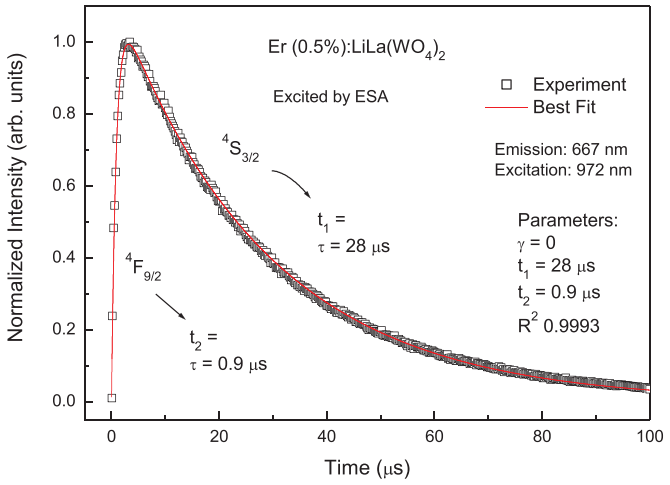

Fig. 4. Emission decay curves measured at 667 nm ($^4F_{9/2} \rightarrow {}^4I_{15/2}$) after laser excitation at 972 nm in Er(0.5%):LiLa$(WO_4)_2$ crystals. The $^4F_{9/2}$ level is excited by the non-radiative decay of the $^4S_{3/2}$ upper level.

Table 2
Best fit luminescence parameters, non-radiative decay and cross-relaxation rates (s^{-1}) for Er^{3+}(0.5%) doped LiLa$(WO_4)_2$ crystal.

Level	γ ($s^{-1/2}$)	τ (expt.) (ms)	τ_d (ms)	τ_R (ms)	W_{NR} (s^{-1})	W_{CR} (s^{-1})	η_ℓ (%)
$^4S_{3/2}$	0	0.039	0.039	0.556	23842	xx	7
$^4F_{9/2}$	0	0.001	0.324	0.324	9.9×10^5	xx	0.3
$^4I_{11/2}$	0	0.150	3.7	3.7	6396	x	4
$^4I_{13/2}$	0	4.2	6.9	6.9	93	x	61

Radiative lifetimes (τ_R) were calculated from Judd-Ofelt theory in this work.
(x) not expected cross-relaxation to occurs. (xx) negligible cross-relaxation effect for $[Er^{3+}] = 0.5$ mol%.

3.3. Non-radiative multiphonon decay

The non-radiative decay rate can be calculated using the decay time constant obtained from the best fit calculations and $W_{NR}(s^{-1}) = \frac{1}{\tau_d} - \frac{1}{\tau_R}$, where τ_d is the intrinsic decay time (without cross-relaxation (CR)) and τ_R is the radiative lifetime calculated from Judd-Ofelt theory (Table 1). The intrinsic decay constant τ_d is equal to the value of parameter t_1 obtained from best fitting of $^4S_{3/2}$ (Fig. 3(a)), $^4I_{13/2}$ (Fig. 3(b)) is equal to τ(expt.) level decay since W_{nr} is observed to be negligible for $[Er^{3+}] = 0.5\%$ for both excited levels. The risetime t_2 in Fig. 3(b) is equal τ(expt.) level decay of the $^4I_{11/2}$ level. The intrinsic luminescence efficiency was calculated using $\eta_\ell = \frac{\tau}{\tau_R}$. Table 2 shows the resulting luminescence decay parameters. It is important to observe that the luminescence decays of the $^4S_{3/2}$ and $^4F_{9/2}$ levels measured are fully exponential (γ = 0); which is a strong indication that multiphonon decay competes with the radiative decay in order to decrease the decays times from 556 μs to 39 μs for the $^4S_{3/2}$ and from 324 μs to 1 μs for the $^4F_{9/2}$ level for $[Er^{3+}] = 0.5\%$.

3.4. Energy transfer up-conversion due to Yb→Er energy transfer

An analysis of the up-conversion process was carried using the 550 nm emission from the $^4S_{3/2}$ level of Er^{3+} produced by excitation of the $^2F_{5/2}$ energy level of Yb^{3+} at 972 nm. Fig. 5 shows the luminescence time transient measured for Yb(x):Er(0.5%):LiLa$(WO_4)_2$ fiber crystals with x = 2, 5, 10 and 15 mol% after pulsed laser excitation under an excitation intensity of 35 MW cm^{-2}. It is observed in Fig. 5 that ESA process occurs for $[Yb^{3+}] < 10$ mol% co-doped samples, i.e. where A_{ESA} (amplitude of the ESA signal) > 0. The best-fit calculations were obtained using an experimental function that precisely describes the luminescence transient given by Eq. (5), which has been used in Ref. [7]

$$I(t) = A_{ESA}\exp(-\gamma_1\sqrt{t_1} - t/t_1) + A_{Up}[\exp(-\gamma_1\sqrt{t} - t/t_1) - \exp(-t/t_2)], \quad (5)$$

where A_{ESA} is the amplitude of the luminescence signal due to ESA absorption and A_{Up} is the amplitude of the up-conversion signal contribution. The fitting parameter t_2 (luminescence rise time) is the up-conversion characteristic time and γ_1 and t_1 are the fitting parameters for the $^4S_{3/2}$ luminescence decay. Best-fit parameters are given in Table 3. The most important information about the rate of up-conversion process is given by the rise time (t_2) that is dependent on the excitation intensity and the increasing (by ytterbium doping) acceptor ($^4S_{3/2}$) lifetime, t_1. ESA contribution that is about 60% of the up-conversion ($^4S_{3/2}$) luminescence signal for Yb^{3+}(2%), decreases to 20% for Yb^{3+}(5%) codoping (see Fig. 5(a) and (b)) and is negligible for $[Yb^{3+}] > 5\%$. Because the up-conversion time (t_2) remains constant (11 μs) for excitation intensities increasing from 28 MW cm^{-2} to 64 MW cm^{-2} we conclude that the rate probability (s^{-1}) for U_{P1} process has already reached its constant value (K_0) according to the critical radius model for ETU process. A critical radius model, which has been presented previously in Ref. [8] explains this observation based on the existence of a critical radius R_C for the ETU interaction, which limitates the ETU rate transfer to constant value for all excited Yb^{3+}-Er^{3+} pairs having a distance separation $R \le R_C$. As a consequence of that model, K_0 is the constant rate for the excitation density $N_{exc} > N_C$, where N_C is the critical concentration of excited donors (Yb^{3+}). Therefore the rate constant of U_{P1} process (ETU) can be calculated from the relation $W_{UP1} = \frac{1}{t_2} - \frac{1}{\tau_d}$ using $t_2 = 11$ μs and $\tau_d = 3.7$ ms (the intrinsic lifetime of donor, $^4I_{11/2}$ level giving a rate constant $W_{Up1} = 90639\ s^{-1}$).

4. Discussion

Results of Fig. 5 have shown a lifetime increasing for the $^4S_{3/2}$ level (Er^{3+}) in Yb^{3+}(x%) co-doped LiLa$(WO_4)_2$ crystals. These lifetime values are given in Table 3. Fig. 6 shows the lifetime dependence on the $[Yb^{3+}]$ concentration. Therefore, the luminescence efficiency of green emission ($^4S_{3/2}$) increases from 7% for $[Yb^{3+}] = 0$ to 36% for $[Yb^{3+}] = 15\%$. This effect must be related to the multiphonon relaxation suppression at Er^{3+} site due to the high excited-state density of Yb^{3+} ions in Yb^{3+}(x):Er^{3+}(0.5) crystal. The phonon diffusion length for low energy phonon or acoustic phonons ℓ_c is approximately equals to 11 Å for tungstate crystals. It is known that Yb^{3+} ion substitution in tungstate lattice introduces local lattice symmetry distortions [9] that affect the thermal conductivity and the phonon length diffusion [10]. It has been observed a thermal conductivity decreasing by factor of three for Yb^{3+}(5%)-doped NaGd$(WO_4)_2$ crystal in comparison to undoped tungstate crystal [10] and the low energy phonon diffusion length decreasing to $\ell_c = 3.7$ Å. Increasing Yb^{3+} concentration, a number of Yb^{3+} symmetry distortions increases, which will decrease the high-phonon energy diffusion abbreviating the phonons breakdown to acoustic phonons and increasing the local bath temperature. This effect associated to the high-energy (~850 cm^{-1}) phonons generated by Yb^{3+} emission sideband in Yb^{3+}(x%):Er^{3+}(0.5%) crystals, may cause the saturation effect of the excited state $^4S_{3/2}$ multiphonon relaxation of Er^{3+} as experimentally observed for Yb^{3+}(x):Er:LiLa$(WO_4)_2$ in this work. A phonon bottleneck (accepting phonon mode saturation) in the multiphonon relaxation process for several singly doped RE^{3+} ions in tellurite, germanate and ZBLAN glasses has been observed and described by Auzel [11]. However, similar effect has never been reported for Er^{3+}($^4S_{3/2}$) luminescence induced by $Yb^{3+} \rightarrow Er^{3+}$ up-conversion. The efficiency of the non-radiative multiphonon decay of an Er^{3+}($^4S_{3/2}$) can be calculated using the expression $\eta_{NR} = W_{nR}(\exp)/W_{nR}(0)$, where W_{nR} *(exp)* is the experimental value that is dependent on the excited state density N_{exc} and W_{nR} *(0)* is the intrinsic nonradiative decay of $^4S_{3/2}$ level (23842 s^{-1}) measured at very low density

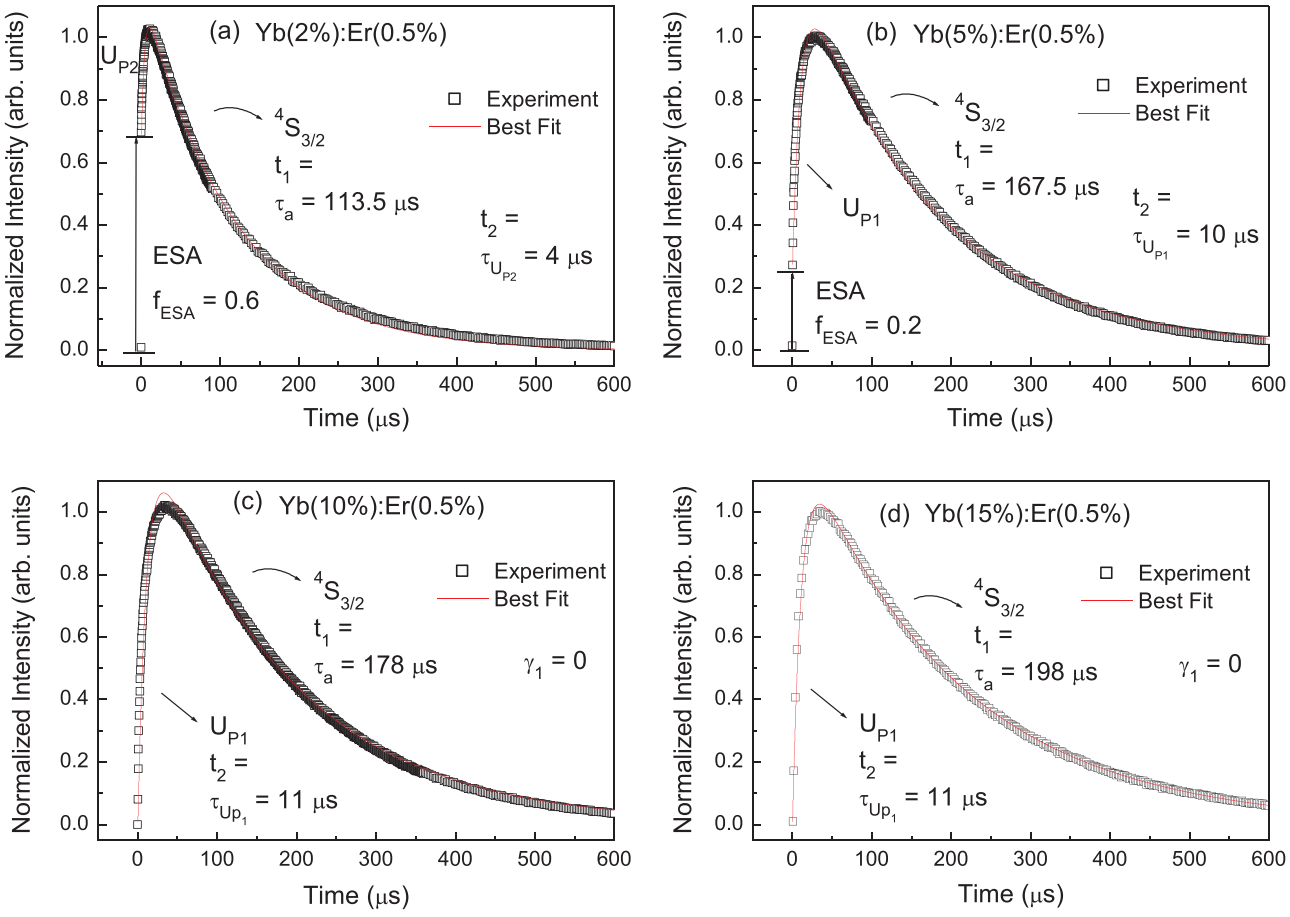

Fig. 5. Measured up-conversion luminescence transient of $^4S_{3/2}$ level measured at 550 nm for Yb(x%):Er(0.5%):LiLa$(WO_4)_2$ fiber crystals (where x = 2, 5, 10 and 15 mol%) after the laser pulse excitation at 972 nm (E = 10 mJ) with an intensity of 35 MW cm^{-2} per pulse. The best-fit calculations are shown in red. The rise time t_2 gives the up-conversion time and t_1 gives the lifetime of $^4S_{3/2}$ level.

Table 3
Best fit luminescence parameters of the luminescence transient of $^4S_{3/2}$ level (up-conversion) for Yb(x%):Er(0.5%):LiLa$(WO_4)_2$ single crystals (fibers). The parameter γ_1 was observed to be zero for all the fittings. η_ℓ is the luminescence efficiency of $^4S_{3/2}$ in Yb^{3+}/Er^{3+} system. The ESA contribution (fraction) is given by $f_{ESA} = A_{ESA}/(A_{ESA}+A_{Up})$.

[Yb] (x mol%)	A_{ESA}	A_{Up}	t_1	t_2	R^2	f_{ESA}	η_ℓ (%)
0	1	0	39 μs	xx	0.999	1	7
2	0.690	0.484	113.5 μs	4 μs	0.998	0.6	20
5	0.265	1.03	167.5 μs	10 μs	0.998	0.2	30
7	0	1	170 μs	11.8 μs	0.997	0	31
10	0	1	178 μs	11 μs	0.997	0	32
15	0	1	198 μs	11 μs	0.999	0	36

(xx) The rise time of luminescence was following the pulse laser excitation as expected for ESA process.
Radiative lifetime of $^4S_{3/2}$ level is τ_R = 556 μs.

excitation intensity. These experimental values of W_{nR} and the respective efficiency η_{nR} measured for many Yb^{3+} excitation densities (N_{exc}) are given in Table 4.

Fig. 7 shows the values of η_{NR} as a function of the excited density of ions (Er^{3+} and Yb^{3+}) by the laser pulse excitation at 972 nm.

The excitation density N_{exc} was calculated for a pulse energy of E = 10 mJ with an excitation volume constant equal to $V = 1.15 \times 10^{-3}$ cm^3 and the absorbance of each Yb(x%):Er(0.5) sample used in the measurements. The effect of reduction of the multiphonon relaxation efficiency for the $^4S_{3/2}$ level (Er^{3+}) with the increasing of the Yb^{3+} concentration (cm^{-3}), observed in Fig. 7, was modeling described assuming the existence of a critical radius R_C, which governs the multiphonon relaxation decay of Er^{3+} according to the following

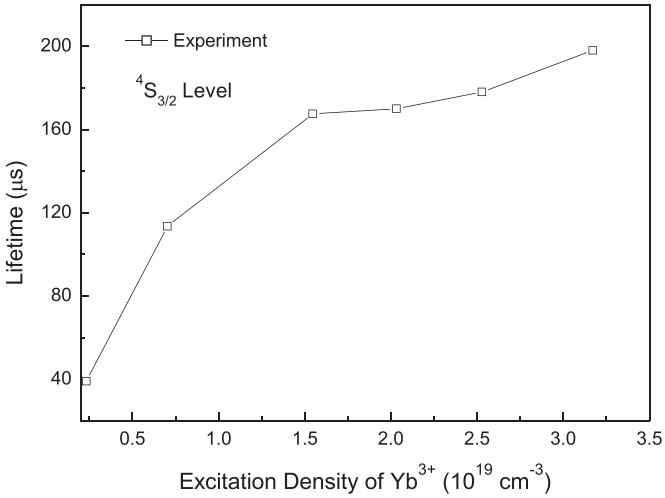

Fig. 6. Measured lifetime of $^4S_{3/2}$ level (Er^{3+}) as a function of the excited density of Yb^{3+}(and Er^{3+}) ions (cm^{-3}) observed after laser excitation at 972 nm in Yb(x%):Er (0.5%):LiLa$(WO_4)_2$ crystals.

assumptions: i) an excited Er^{3+} ion that has an excited Yb^{3+} ion inside of a volume defined by the critical radius R_C will have a multiphonon relaxation efficiency equal to 1 (η_{NR} = 1) only for the high-energy (~800 cm^{-1}) phonons generation (at Er^{3+} site) propagating in the opposite direction linking both Er^{3+} and Yb^{3+} excited ions (or (-z) direction). Nevertheless, the multiphonon relaxation decay will have efficiency equal to zero (η_{NR} = 0) for phonons generation propagating in

Table 4
Multiphonon decay rate values for the $^4S_{3/2}$ level of Er^{3+} measured for many excitation density of Yb^{3+} in Yb(x%): Er(0.5%):LiLa$(WO_4)_2$ crystals.

N_{exc} (cm^{-3})	[Yb^{3+}] (mol%)	W_{NR} (s^{-1})	η_{nR}
5×10^{17}	0	23842	1
7.04×10^{18}	2	7012	0.294
1.55×10^{19}	5	4172	0.175
2.03×10^{19}	7	4085	0.171
2.53×10^{19}	10	3819	0.160
3.17×10^{19}	15	3252	0.136

Non-radiative multiphonon efficiency was taken relatively to the intrinsic value obtained for single doped Er^{3+}(0.5%) crystal under low excitation density.

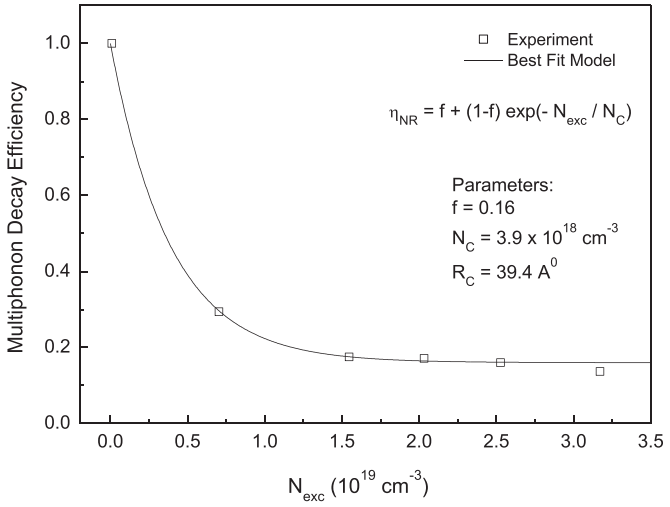

Fig. 7. Effect on the multiphonon relaxation efficiency for the $^4S_{3/2}$ level (Er^{3+}) as a function of the Yb^{3+} concentration (cm^{-3}) observed after laser excitation at 972 nm in Yb(x%):Er(0.5%):LiLa$(WO_4)_2$ crystals. Best fit was performed using the critical radius model.

all different (x), (-x), (y), (-y) and (z) directions; ii) an excited Er^{3+} ion having an excited Yb^{3+} ion outside of critical volume V_C will have an unchanged multiphonon relaxation process with $\eta_{NR}=1$. Assuming a random distribution between Er^{3+} and Yb^{3+} ions in the lattice one has the following equation, which was firstly obtained in the exponential form to describe the interaction between an excited F center and the OH^- molecule in KCl [12].

$$\eta_{NR} = f + (1-f)\exp(-N_{exc}/N_C), \quad (6)$$

where N_{exc} is the excited concentration of Yb^{3+}(cm^{-3}) ions and N_C is the critical concentration of excited Yb^{3+} ions; f is the fraction of excited Er^{3+} ions having the intrinsic multiphonon relaxation unchanged, besides the presence of an excited Yb^{3+} inside of a critical volume V_C. Fig. 7 shows that the experimental results can be best fitted using the Eq. (6) derived from the critical radius model giving $f=0.16$ and N_C equal to 3.9×10^{18} cm^{-3}. A critical radius of $R_C=39.4$ Å is obtained. One must to observe that the fraction $f=0.16$ is very close to ratio value 1/6 that is consistent with the initial assumption that only multiphonons generation (Er^{3+}) propagating at (-z) direction do not feel the acceptor mode saturation produced by phonon emission sideband of Yb^{3+} inside of the critical interaction volume. The critical radius experimentally obtained is about 3.6 times larger than the diffusion length of the low phonon energy (acoustic phonons) $\ell_c=11$ Å estimated for tungstate crystals using the following equation

$$\ell_c = \frac{3k}{C_P v_s}, \quad (7)$$

where the thermal conductivity (k), the specific heat (C_P) and the sound velocity (v_s) values were obtained for $KLu(WO_4)_2$ crystal [10].

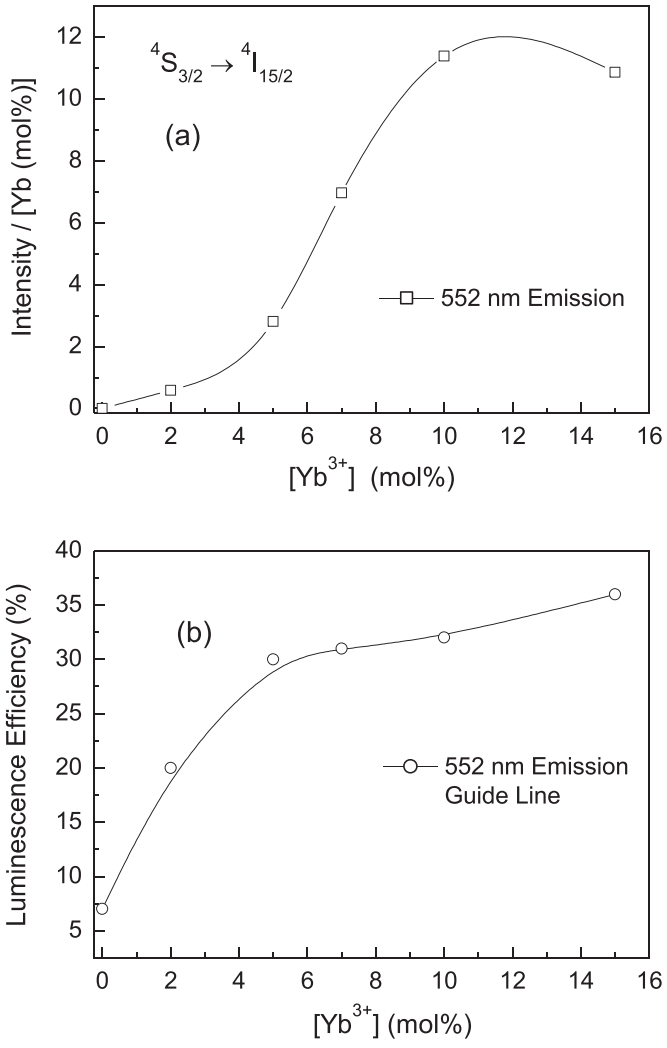

Fig. 8. Normalized up-conversion emission intensity (a) and the luminescence efficiency (b) of $^4S_{3/2}$ level (Er^{3+}) plotted as a function of Yb^{3+} concentration for Yb(x%):Er(0.5%):LiLa$(WO_4)_2$ crystals.

4.1. Best concentration for Yb^{3+}(x)→Er^{3+} up-conversion

Fig. 8(a) shows the normalized intensity, which was obtained dividing it by [Yb^{3+}] concentration (mol%), of $^4S_{3/2}$ up-conversion emission at 552 nm plotted as a function of [Yb^{3+}] concentration for Yb(x%):Er(0.5%):LiLa$(WO_4)_2$ crystals. Fig. 8(b) shows the luminescence efficiency (η_ℓ) of $^4S_{3/2}$ up-conversion emission as a function of the Yb^{3+} concentration (using the data of Table 3). Besides the luminescence efficiency showed small increase for [Yb^{3+}]=15 mol%, the optimization of the green up-conversion emission in Yb:Er:LiLa$(WO_4)_2$ crystal is obtained by observing the intensity curve of Fig. 8(a) that exhibits a maximum intensity for [Yb^{3+}] equals to 11.5 mol%. Numerical solution of the rate equations is carrying out to characterize the potential for laser emission at 552 nm. The calculated evolution of the population inversion (n_4-n_3), in mol% obtained by numerical simulation of the rate equations for [Yb^{3+}]=10 mol% using several pumping rates for a continuous regime at 972 nm pump rates is already in course.

5. Conclusions

The intrinsic luminescence efficiency of the $^4S_{3/2}$→$^4I_{15/2}$ transition with a peak wavelength of 552 nm in Er^{3+}-doped LiLa$(WO_4)_2$ crystal was determined to be 7%; a value reduced from the radiative lifetime because of strong multiphonon emission process. We observed that the

decay time of the $^4S_{3/2}$ level in Yb:Er:LiLa$(WO_4)_2$ crystal increases with the [Yb^{3+}] concentration reaching the value of 198 μs and a luminescence efficiency of 36% for Yb^{3+} doping with 15 mol%. This result suggests a phonon bottleneck in the multiphonon relaxation process of the $^4S_{3/2}$ level due to the presence of an excited Yb^{3+} ion inside of a critical radius of $R_C = 39.4$ Å. The observation of the $Yb^{3+} \rightarrow Er^{3+}$ energy transfer has shown that ESA process dominates the up-conversion luminescence from $^4S_{3/2}$ level for [Yb^{3+}] ≤ 2 mol%. However, $Yb^{3+} \rightarrow Er^{3+}$ energy transfer up-conversion (ETU) process dominates the visible up-conversion luminescence for [Yb^{3+}] ≥ 5 mol% and none ESA effect is observed for [Yb^{3+}] ≥ 10 mol%. We established that the green up-conversion luminescence of Er^{3+} is optimized using an Yb^{3+} concentration of 11.5 mol% for Er^{3+}(0.5%):LiLa$(WO_4)_2$ crystal.

Acknowledgments

The authors thank financial support from São Paulo State Research Foundation (FAPESP, Grants No. 1995/4166-0 and 2000/10986-0), Brazilian Research Foundation (CNPq, grants No. 465763/2014-6 and 308736/2014-1).

References

[1] P.E.A. Mobert, E. Heumann, G. Huber, B.H.T. Chai, Opt. Lett. 22 (18) (1997) 1412.
[2] R. Brede, E. Heumann, J. Koetke, T. Danger, G. Huber, B.H.T. Chai, Appl. Phys. Lett. 63 (15) (1993) 2030.
[3] J.R. de Moraes, S.L. Baldochi, L.R.L. Soares, V.L. Mazzocchi, C.B.R. Parente, L.C. Courrol, Mater. Res. Bull. 47 (2012) 744–749.
[4] X.Y. Huang, Z.B. Lin, L.Z. Zhang, G.F. Wang, Mater. Res. Innov. 12 (2) (2008) 94.
[5] M.J. Weber, Phys. Rev. 157 (2) (1967) 262.
[6] A.I. Burshtein, Sov. JETP 35 (1972) 882.
[7] L.D. da Vila, L. Gomes, L.V.G. Tarelho, S.J.L. Ribeiro, Y. Messaddeq, J. Appl. Phys. 93 (2003) 3873.
[8] S.D. Jackson, A.F.H. Librantz, F.H. Jagosich, L. Gomes, G. Poirier, S.J.L. Ribeiro, Y. Messaddeq, J. Appl. Phys. 101 (2007) 123111.
[9] J.M. Postema, W.T. Fu, D.J.W. Ijdo, J. Solid State Chem. 184 (2011) 2004.
[10] Jiandong Fan, Huaijin Zhang, Jiyang Wang, Zongcheng Ling, HairuiXia, Xiufang Chen, Yonggui Yu, Qingming Lu, Minhua Jiang, J. Phys. D: Appl. Phys. 39 (2006) 1034.
[11] F. Pellé, N. Gardant, F. Auzel, J. Opt. Soc. Am. B 15 (2) (1998) 667.
[12] L. Gomes, F. Luty, Phys. Rev. B 30 (12) (1984) 7194.